Published in final edited form as:
Science. 2012 May 25; 336(6084): 1040–1044. doi:10.1126/science.1218595.

Metabolite Profiling Identifies a Key Role for Glycine in Rapid Cancer Cell Proliferation

Mohit Jain[1,2,3,4,*], **Roland Nilsson**[1,2,3,5,*], **Sonia Sharma**[6], **Nikhil Madhusudhan**[1,2,3], **Toshimori Kitami**[1,2,3], **Amanda L. Souza**[1], **Ran Kafri**[2], **Marc W. Kirschner**[2], **Clary B. Clish**[1], and **Vamsi K. Mootha**[1,2,3]

[1]Broad Institute, Cambridge, Massachusetts 02142, USA

[2]Department of Systems Biology, Harvard Medical School, Boston, Massachusetts 02115, USA

[3]Center for Human Genetic Research and Department of Molecular Biology, Massachusetts General Hospital, Boston, Massachusetts 02114, USA

[4]Division of Cardiovascular Medicine, Department of Medicine, Brigham and Women's Hospital, Boston, Massachusetts 02115, USA

[5]Unit of Computational Medicine, Department of Medicine, Karolinska Institutet, 17176 Stockholm, Sweden

[6]La Jolla Institute for Allergy & Immunology, La Jolla, California 92037, USA

Abstract

Metabolic reprogramming has been proposed to be a hallmark of cancer, yet we currently lack a systematic characterization of the metabolic pathways active in transformed cells. Using mass spectrometry, we measured the consumption and release (CORE) of 219 metabolites from media across the NCI-60 cancer cell lines, and integrated CORE profiles with a pre-existing atlas of gene expression. The integrated analysis identified glycine consumption and expression of the mitochondrial glycine biosynthetic pathway as strongly correlated with rates of proliferation across cancer cells. Antagonizing glycine uptake and its mitochondrial biosynthesis preferentially impaired rapidly proliferating cells. Moreover, higher expression of this pathway was associated with greater mortality in breast cancer patients. Increased reliance on glycine may represent a metabolic vulnerability for selectively targeting rapid cancer cell proliferation.

Malignant transformation results from mutations that alter cellular physiology to confer a proliferative advantage (1, 2). Despite the genetic heterogeneity and complexity of cancer (3), transformed cells exhibit a number of proposed common hallmarks, including metabolic

Address Correspondence to: Vamsi K. Mootha, M.D., MGH Department of Molecular Biology, 185 Cambridge Street 6th Floor, Boston, MA 02114 USA, vamsi@hms.harvard.edu.
*These authors contributed equally to this work.

Author Contributions

M.J. and R.N. conceived of and performed all experiments, collected and analyzed experimental data, and prepared the manuscript. S.S. assisted with cell culture, RNAi and T lymphocyte experiments. N.M. and T.K. assisted with cell culture and imaging based experiments. A.S. and C.B.C. performed LC-MS/MS profiling experiments and provided experimental feedback. R.K. and M.W.K. performed cell cycle studies. V.K.M conceived of all experiments, reviewed all experimental data and prepared the manuscript. M.J. and R.N. contributed equally to this work. All authors have discussed the results and reviewed the manuscript.

All authors declare no competing financial interests.

The full metabolite CORE profiling dataset is available in the Supporting Online Material (www.sciencemag.org) as well as through the NCI Molecular Targets data repository (http://dtp.nci.nih.gov/mtargets/download.html).

reprogramming, which manifests as altered nutrient uptake and utilization (2, 4). Although metabolic reprogramming is thought to be essential for rapid cancer cell proliferation, a systematic characterization of the metabolic pathways active in transformed cells is lacking, and the contribution of these pathways in promoting rapid cancer cell proliferation remains unclear (4). Existing studies of cancer metabolism have only examined relatively few cell lines, and have largely focused on measurement of intracellular metabolite pools (5) from which it is difficult to infer metabolic pathway activity, or have estimated metabolic flux through a limited number of reactions using isotope tracing (6).

To systematically characterize cancer cell metabolism, we used liquid chromatography-tandem mass spectrometry to profile the cellular consumption and release (CORE) of 219 metabolites (table S1) spanning the major pathways of intermediary metabolism, in the NCI-60 panel, a collection of sixty well-characterized primary human cancer cell lines established from nine common tumor types (7). CORE profiling builds upon metabolic footprinting or exometabolomics (8, 9), and provides a systematic and quantitative assessment of cellular metabolic activity by relating metabolite concentrations in medium from cultured cells to baseline medium, resulting in a time-averaged consumption and release (CORE) profile for each metabolite on a per cell basis over a period of exponential growth (Fig. 1). Using CORE profiling we identified 140 metabolites that were either present in fresh medium or released by at least one cancer cell line, of which 111 metabolites demonstrated appreciable variation across the 60 cell lines, with excellent reproducibility between biological replicates (Fig. 2). Approximately one third of the 111 metabolites were consumed by all cell lines, whereas most of the remaining two thirds of metabolites were consistently released into the medium; only a handful of metabolites exhibited consumption in certain cell lines and release by others (Fig. 2). A larger, fully annotated version of Fig. 2 is provided in Fig. S1.

This CORE atlas of cancer metabolism (Fig. 2, S1) can be used to explore metabolic phenotypes of cancer cells and to discover relationships between metabolites. For example, ornithine was released from leukemia cells and adenosine and inosine were released from melanoma cells (Fig. S2), reflecting metabolic activities that may be unique to these cancers. Unsupervised cluster analysis of metabolite CORE data identified leukemia cells as a distinct group, but did not more generally distinguish between tumor cell lines based on tissue of origin (Fig. S3). Functionally related metabolites demonstrated similar patterns of consumption and release across the 60 cell lines. For example, major nutrients including glucose, essential amino acids, and choline formed a single cluster, as did metabolites representing glycolysis, the citric acid cycle, nucleotides, and polyamines (Fig. 2, Fig. S1). Consumption of major nutrients also correlated with release of their byproducts: for example, glucose consumption correlated to lactate release (Fig. 1B), consistent with the well-documented Warburg effect in transformed cells (4). A similar pattern of nutrient consumption and byproduct release was also observed with other nutrients. Glutamine consumption, quantitatively the greatest among amino acids, was closely mirrored by glutamate release (Fig. 1B). An analysis of all monitored metabolites revealed that total measured carbon consumption was also closely correlated to total measured carbon release (Fig. 1B), suggesting that transformed cells share a common metabolic phenotype of incomplete catabolism of major nutrients followed by byproduct release.

We next sought to determine whether any metabolite CORE profiles were associated with cancer cell proliferation. Previously reported doubling times across the 60 cancer cell lines ranged from 17.0 to 79.5 hours and were highly reproducible (10)(Fig. S4). From the 111 metabolite CORE profiles, two metabolites, phosphocholine and glycine, were significantly correlated (Bonferroni-corrected $P < 0.01$) with proliferation rate across the 60 cell lines (Fig. 3A). Phosphocholine, which was released from all cells, correlated with consumption

of the essential nutrient choline (Fig. S5), and has been reported to accumulate in transformed cells as a substrate for phospholipid biosynthesis (11). In contrast, the relation between glycine consumption and proliferation rate was unanticipated, since glycine is a non-essential amino acid that can be endogenously synthesized. Glycine exhibited an unusual CORE profile, being consumed by rapidly proliferating cells and released by slowly proliferating cells (Fig. 3B), suggesting that glycine demand may exceed endogenous synthesis capacity in rapidly proliferating cancer cells, whereas in slowly proliferating cells, glycine synthesis may exceed demand. Increasing glyine consumption with faster proliferating rate was observed across all 60 cell lines (Fig. 3B), and was even more pronounced within specific tumor types, including ovarian, colon, and melanoma cells (Fig. 3B, Fig. S6), but not evident in non-adherent leukemia cells (Fig. S6). To determine whether glycine consumption is specific to transformed cells or a general feature of rapid proliferation, we measured glycine consumption in cultured primary human mammary epithelial cells (HMEC), human bronchial epithelial cells (HBE), human umbilical vein endothelial cells (HUVEC) and human activated CD4+ T lymphocytes. These nontransformed cells had doubling times between 8 and 18 hours, comparable to the most rapidly dividing cancer cells, yet each of these cell types released rather than consumed glycine (HMEC: 3.5 ± 0.8; HBE 17.5 ± 3.2; HUVEC 8.4 ± 1.4; lymphocytes 1.9 ± 0.3 fmol/cell/h). Thus, glycine consumption appears to be a feature specific to rapidly proliferating transformed cells.

To complement the metabolite CORE analysis, we next examined the gene expression of 1,425 metabolic enzymes (12) in a previously generated microarray dataset across these 60 cell lines (13). This independent analysis revealed that glycine biosynthesis enzymes are more highly expressed in rapidly proliferating cancer cell lines (Fig. 3C). Intracellular glycine synthesis is compartmentalized between the cytosol and mitochondria (14), providing two separate enzymatic pathways (Fig. 3D). The mitochondrial glycine synthesis pathway consists of the glycine-synthesizing enzyme serine hydroxymethyltransferase 2, *SHMT2*, a target of the oncogene c-Myc (15), as well as *MTHFD2* and *MTHFD1L*, which regenerate the cofactor tetrahydrofolate (THF) for the SHMT2 reaction (Fig. 3D). Only the mitochondrial pathway exhibited significant correlation with proliferation, whereas the corresponding cytosolic enzymes did not (Fig. 3C), suggesting a key role for mitochondria in supporting rapid cancer cell proliferation. To assess the relative contributions of glycine consumption *vs.* endogenous synthesis to intracellular glycine pools, we utilized tracer analysis with ^{13}C-labeled glycine in rapidly dividing LOX IMVI cells. Assuming a simple steady state model (13), we estimate from labeling of intracellular glycine and serine pools (Fig. 3E) that approximately one-third of intracellular glycine originates from extracellular consumption, whereas the remainder is synthesized endogenously. Thus, both metabolite CORE profiling and gene expression analysis independently identify glycine metabolism as closely related to rapid proliferation in cancer cells.

To directly evaluate the contribution of glycine metabolism to rapid cancer cell proliferation, we used a combination of genetic silencing and nutrient deprivation. We stably silenced expression of the glycine-synthesizing enzyme *SHMT2* in slowly proliferating A498 cells and in rapidly proliferating LOX IMVI cells (Fig. 3B) with four distinct shRNA hairpins (Fig. S7A). CHO strains mutant in SHMT2 have previously been shown to be auxotrophic for glycine (16). Silencing of SHMT2 in the absence of extracellular glycine halted proliferation of LOX IMVI cells (Fig. 3F), and was rescued by the addition of glycine to the medium, indicating that glycine itself, rather than one-carbon units derived from the SHMT2 reaction (Fig. 3D), is critical to proliferation in these cells (Fig. 3F). Supplementation of medium with sarcosine, a glycine-related metabolite (17), or formate, a source of cellular one-carbon units (18), failed to rescue LOX IMVI cells (Fig. S7B). In contrast, slowly proliferating A498 cells (Fig. 3F) were not impaired by *SHMT2* depletion and extracellular

glycine deprivation, indicating that other means of glycine synthesis can satisfy the requirements in these cells. Withdrawal of extracellular glycine alone also reduced the proliferation of LOX IMVI cells but not A498 cells (Fig. S8), although this effect was more subtle. Collectively, our data suggest that mitochondrial production of glycine is critical specifically in rapidly proliferating cancer cells. To determine whether this reliance on glycine for rapid proliferation extends to other cancer cells, we tested silencing of *SHMT2* (Fig. S7C) and extracellular glycine deprivation of 10 additional primary cancer cell lines from the NCI-60 panel (Fig. 3G). Rapidly proliferating cancer cells exhibited slower proliferation with antagonism of glycine metabolism and were rescued with addition of extracellular glycine, whereas slowly proliferating cells were less sensitive to these perturbations (Fig. 3G), even when assessed at later time points to allow for a comparable number of cellular divisions relative to rapidly proliferating cells (Fig. S9).

We next sought to explore the potential mechanisms by which glycine metabolism contributes to rapid cancer cell proliferation. Metabolic tracing with ^{13}C-labeled glycine revealed incorporation of consumed glycine into purine nucleotides in rapidly proliferating LOX IMVI cells, but limited incorporation in slowly proliferating A498 cells (Fig. 4A,B), suggesting that consumed glycine in part supports *de novo* purine synthesis in these cells. We also noted incorporation of labeled glycine into cellular glutathione (Fig. S10A). Analysis of previously performed large scale chemosensitivity profiling across the 60 cancer cells (7) revealed that sensitivity to an inhibitor of glutathione synthesis, buthionine sulfoximine (19), was unrelated to proliferation rate (Fig. S10B), whereas sensitivity to inhibitors of *de novo* purine biosynthesis, mycophenolate, tiazofurin, and alanosine (20), were highly correlated with proliferation rate across the cell lines (Fig. S10C). Glycine can be utilized for *de novo* purine biosynthesis by two mechanisms, direct incorporation into the purine backbone or further oxidation by the glycine cleavage system (GCS) to yield one-carbon units for nucleotide synthesis and cellular methylation reactions (Fig. 4A). Since only carbon 2 of glycine is converted into one-carbon units by the GCS (Fig. 4A), we cultured LOX cells in 1-^{13}C-glycine or 2-^{13}C-glycine to differentiate between these two mechanisms (21). Consumed 2-^{13}C-glycine did not give rise to doubly labeled purines (Fig. 4B), indicating that the incorporation of consumed glycine into purine nucleotides does not involve oxidation by the GCS. To better characterize the impact of glycine deprivation on cell cycle progression, we performed cell cycle analysis in HeLa cancer cells expressing a geminin-GFP reporter and stained with DAPI (4′,6-diamidino-2-phenylindole). Silencing of SHMT2 (Fig. S11A) and deprivation of extracellular glycine slowed proliferation in HeLa cells (Fig. S11B), similar to other fast proliferating cancer cells (Fig. 3G), and resulted in prolongation of G_1 phase of the cell cycle (Fig. 4C, S11C), while protein synthesis remained relatively intact (Fig. S11D), consistent with a defect in nucleotide biosynthesis (20). Collectively, these results suggest that consumed glycine is utilized in part for *de novo* purine nucleotide biosynthesis in rapidly proliferating in these cells, and antagonism of glycine metabolism results in prolongation of G_1, thus slowing proliferation.

To explore the potential relevance of glycine metabolism to cancer, we examined the expression of the mitochondrial glycine synthesis enzymes, *SHMT2*, *MTHFD2* and *MTHFD1L* (Fig. 3D), in previously generated microarray datasets across six independent large cohorts totaling over 1300 patients with early stage breast cancer followed for survival (22–27). We defined two groups of individuals: those with above-median gene expression of the mitochondrial glycine biosynthesis pathway, and those with below-median gene expression. Above-median expression of the mitochondrial glycine biosynthesis pathway was associated with greater mortality (Fig. 5), and a formal meta-analysis of all six datasets indicated an overall hazard ratio of 1.82 (95% CI: 1.43 – 2.31; Fig. 5), comparable to that of other established factors such as lymph node status and tumor grade, that contribute to poor cancer prognosis (25). The mitochondrial glycine synthesis enzyme *SHMT2* alone was also

significantly associated with mortality, whereas its cytosolic paralog *SHMT1* was not (Fig. S12). These data highlight the potential importance of mitochondrial glycine metabolism in human breast cancer.

In summary, we have generated a large-scale, quantitative atlas of cancer cell metabolism using CORE profiling. This methodology and dataset may be of broad utility for investigating cellular metabolism, as well as for identifying metabolite biomarkers of cancer and drug responsiveness. In the current study, we have utilized this atlas to probe the relation between metabolism and proliferation to discover an unexpected increased reliance on glycine metabolism in rapid proliferation cancer cells, a phenotype that was not observed in rapidly proliferating nontransformed cells. While we find that glycine is utilized for *de novo* purine nucleotide biosynthesis in rapidly proliferating LOX IMVI cells, alternative mechanisms including utilization of one-carbon groups derived from glycine for cellular methylation reactions (17), may be important in other cancer cell types. Importantly, recent work has identified that glycine and related metabolites, including sarcosine, serine and threonine, or their associated metabolic pathways, are central to cancer metastasis (5), cellular transformation (17, 28, 29), and murine embryonic stem cell proliferation (30). Glycine metabolism may therefore represent a metabolic vulnerability in rapidly proliferating cancer cells that could in principle be targeted for therapeutic benefit.

Methods summary

For detailed description of methods, please see Supplemental Methods.

Briefly, NCI-60 cancer cell lines were cultured in according to prior specifications (7), and media samples were collected at baseline and after 4–5 days in culture. Metabolites were measured in medium using LC-MS/MS, and absolute concentrations were determined using serial dilutions of standards covering physiologic concentration ranges. Metabolite CORE profiles were determined for each metabolite and cell line by examining the change in metabolite concentration from fresh medium to spent medium, calculating the molar difference, and normalizing to the area under the growth curve for the corresponding cell line, to yield a metabolite consumption or release value/cell/hr. SHMT2 was silenced in cell lines through stable expression of one of four shRNAs targeting distinct sequences for human SHMT2 (sh1-4) or a control shRNA (shCtrl). Tracer studies were performed using stable isotope ^{13}C-glycine labeled in the carbon 1 versus carbon 2 position. Cell cycle analysis was performed in HeLa cells expressing a reporter construct for geminin and stained for DNA and protein content. *In-vitro* doubling times and tissue type annotations for NCI-60 cells were provided by the NCI (http://dtp.nci.nih.gov/docs/misc/common_files/cell_list.html). Previously generated microarray analysis and compound sensitivity measures for small molecules across the NCI-60 were obtained from the NCI data repository (http://dtp.nci.nih.gov/docs/dtp_search.html). For details of statistical analyses and expanded details for above experiments please see Supplementary Materials and Methods.

Supplementary Material

Refer to Web version on PubMed Central for supplementary material.

Acknowledgments

The authors thank Todd R Golub, Oded Shaham, Scott B Vafai and Laura Strittmatter for scientific discussions and feedback; Xin Cao for assistance with glucose and lactate measurements; the Broad Institute RNAi Platform for shRNA reagents; David Gomez-Cabrero for assistance with multidimensional scaling; Alexander Ploner and Paul Dickman for assistance with survival analysis; William C Kopp, Susan L Holbeck, Katherine Gill, and Penny Sellers of the Developmental Therapeutics Program, National Cancer Institute for reagents and assistance with cell culture; and Tom Hasaka of the Broad Institute for assistance with imaging studies. M.J. was supported by NIH

K08HL107451; R.N. was supported by a postdoctoral scholarship from the Knut & Alice Wallenberg Foundation and Stockholm County (SLL) grant 01626-2009; S.S. was supported by a Special Fellow award from the Lymphoma & Leukemia Society. This work was funded by grants from the NIH R01DK081457 and a gift from the Nestle Research Center (V.K.M).

References

1. Nowell PC. The clonal evolution of tumor cell populations. Science. 1976; 194:23. [PubMed: 959840]
2. Hanahan D, Weinberg RA. Hallmarks of cancer: the next generation. Cell. 2011; 144:646. [PubMed: 21376230]
3. Stratton MR, Campbell PJ, Futreal PA. The cancer genome. Nature. 2009; 458:719. [PubMed: 19360079]
4. Hsu PP, Sabatini DM. Cancer cell metabolism: Warburg and beyond. Cell. 2008; 134:703. [PubMed: 18775299]
5. Sreekumar A, et al. Metabolomic profiles delineate potential role for sarcosine in prostate cancer progression. Nature. 2009; 457:910. [PubMed: 19212411]
6. DeBerardinis RJ, et al. Beyond aerobic glycolysis: transformed cells can engage in glutamine metabolism that exceeds the requirement for protein and nucleotide synthesis. Proc Natl Acad Sci U S A. 2007; 104:19345. [PubMed: 18032601]
7. Shoemaker RH. The NCI60 human tumour cell line anticancer drug screen. Nat Rev Cancer. 2006; 6:813. [PubMed: 16990858]
8. Allen J, et al. High-throughput classification of yeast mutants for functional genomics using metabolic footprinting. Nat Biotechnol. 2003; 21:692. [PubMed: 12740584]
9. Shaham O, et al. A plasma signature of human mitochondrial disease revealed through metabolic profiling of spent media from cultured muscle cells. Proc Natl Acad Sci U S A. 2010; 107:1571. [PubMed: 20080599]
10. O'Connor PM, et al. Characterization of the p53 tumor suppressor pathway in cell lines of the National Cancer Institute anticancer drug screen and correlations with the growth-inhibitory potency of 123 anticancer agents. Cancer Res. 1997; 57:4285. [PubMed: 9331090]
11. Katz-Brull R, Degani H. Kinetics of choline transport and phosphorylation in human breast cancer cells; NMR application of the zero trans method. Anticancer Res. 1996; 16:1375. [PubMed: 8694504]
12. Duarte NC, et al. Global reconstruction of the human metabolic network based on genomic and bibliomic data. Proc Natl Acad Sci U S A. 2007; 104:1777. [PubMed: 17267599]
13. Materials and methods are available as supplementary material on *Science* Online.
14. Tibbetts AS, Appling DR. Compartmentalization of Mammalian folate-mediated one-carbon metabolism. Annu Rev Nutr. 2010; 30:57. [PubMed: 20645850]
15. Nikiforov MA, et al. A functional screen for Myc-responsive genes reveals serine hydroxymethyltransferase, a major source of the one-carbon unit for cell metabolism. Mol Cell Biol. 2002; 22:5793. [PubMed: 12138190]
16. Kao F, Chasin L, Puck TT. Genetics of somatic mammalian cells. X. Complementation analysis of glycine-requiring mutants. Proc Natl Acad Sci U S A. 1969; 64:1284. [PubMed: 5271752]
17. Zhang WC, et al. Glycine decarboxylase activity drives non-small cell lung cancer tumor-initiating cells and tumorigenesis. Cell. 2012; 148:259. [PubMed: 22225612]
18. Patel H, Pietro ED, MacKenzie RE. Mammalian fibroblasts lacking mitochondrial NAD+-dependent methylenetetrahydrofolate dehydrogenase-cyclohydrolase are glycine auxotrophs. J Biol Chem. 2003; 278:19436. [PubMed: 12646567]
19. Griffith OW, Meister A. Potent and specific inhibition of glutathione synthesis by buthionine sulfoximine (S-n-butyl homocysteine sulfoximine). J Biol Chem. 1979; 254:7558. [PubMed: 38242]
20. Linke SP, Clarkin KC, Di Leonardo A, Tsou A, Wahl GM. A reversible, p53-dependent G0/G1 cell cycle arrest induced by ribonucleotide depletion in the absence of detectable DNA damage. Genes Dev. 1996; 10:934. [PubMed: 8608941]

21. Fu TF, Rife JP, Schirch V. The role of serine hydroxymethyltransferase isozymes in one-carbon metabolism in MCF-7 cells as determined by (13)C NMR. Arch Biochem Biophys. 2001; 393:42. [PubMed: 11516159]
22. Chin K, et al. Genomic and transcriptional aberrations linked to breast cancer pathophysiologies. Cancer Cell. 2006; 10:529. [PubMed: 17157792]
23. Desmedt C, et al. Strong time dependence of the 76-gene prognostic signature for node-negative breast cancer patients in the TRANSBIG multicenter independent validation series. Clin Cancer Res. 2007; 13:3207. [PubMed: 17545524]
24. Pawitan Y, et al. Gene expression profiling spares early breast cancer patients from adjuvant therapy: derived and validated in two population-based cohorts. Breast Cancer Res. 2005; 7:R953. [PubMed: 16280042]
25. van de Vijver MJ, et al. A gene-expression signature as a predictor of survival in breast cancer. N Engl J Med. 2002; 347:1999. [PubMed: 12490681]
26. Kao KJ, Chang KM, Hsu HC, Huang AT. Correlation of microarray-based breast cancer molecular subtypes and clinical outcomes: implications for treatment optimization. BMC Cancer. 2011; 11:143. [PubMed: 21501481]
27. Miller LD, et al. An expression signature for p53 status in human breast cancer predicts mutation status, transcriptional effects, and patient survival. Proc Natl Acad Sci U S A. 2005; 102:13550. [PubMed: 16141321]
28. Possemato R, et al. Functional genomics reveal that the serine synthesis pathway is essential in breast cancer. Nature. 2011; 476:346. [PubMed: 21760589]
29. Locasale JW, et al. Phosphoglycerate dehydrogenase diverts glycolytic flux and contributes to oncogenesis. Nat Genet. 2011; 43:869. [PubMed: 21804546]
30. Wang J, et al. Dependence of mouse embryonic stem cells on threonine catabolism. Science. 2009; 325:435. [PubMed: 19589965]
31. Alpert AJ. Hydrophilic-interaction chromatography for the separation of peptides, nucleic acids and other polar compounds. J Chromatogr. 1990; 499:177. [PubMed: 2324207]
32. Luo B, Groenke K, Takors R, Wandrey C, Oldiges M. Simultaneous determination of multiple intracellular metabolites in glycolysis, pentose phosphate pathway and tricarboxylic acid cycle by liquid chromatography-mass spectrometry. J Chromatogr A. 2007; 1147:153. [PubMed: 17376459]
33. Eisen MB, Spellman PT, Brown PO, Botstein D. Cluster analysis and display of genome-wide expression patterns. Proc Natl Acad Sci U S A. 1998; 95:14863. [PubMed: 9843981]
34. de Leeuw J, Mair P. Multidimensional Scaling Using Majorization: SMACOF in R. Journal of Statistical Software. 2009; 31
35. Rantanen A, Rousu J, Kokkonen JT, Tarkiainen V, Ketola RA. Computing positional isotopomer distributions from tandem mass spectrometric data. Metab Eng. 2002; 4:285. [PubMed: 12646323]
36. Zamboni N, Fendt SM, Ruhl M, Sauer U. (13)C-based metabolic flux analysis. Nat Protoc. 2009; 4:878. [PubMed: 19478804]
37. Moffat J, et al. A lentiviral RNAi library for human and mouse genes applied to an arrayed viral high-content screen. Cell. 2006; 124:1283. [PubMed: 16564017]
38. Subramanian A, et al. Gene set enrichment analysis: a knowledge-based approach for interpreting genome-wide expression profiles. Proc Natl Acad Sci U S A. 2005; 102:15545. [PubMed: 16199517]
39. Sakaue-Sawano A, et al. Visualizing spatiotemporal dynamics of multicellular cell-cycle progression. Cell. 2008; 132:487. [PubMed: 18267078]
40. Toettcher JE, et al. Distinct mechanisms act in concert to mediate cell cycle arrest. Proc Natl Acad Sci U S A. 2009; 106:785. [PubMed: 19139404]
41. Cox DR. Regression models and life-tables. Journal of the Royal Statistical Society Series B. 1972; 34:187.
42. Bland JM, Altman DG. The logrank test. BMJ. 2004; 328:1073. [PubMed: 15117797]
43. DerSimonian R, Laird N. Meta-analysis in clinical trials. Control Clin Trials. 1986; 7:177. [PubMed: 3802833]

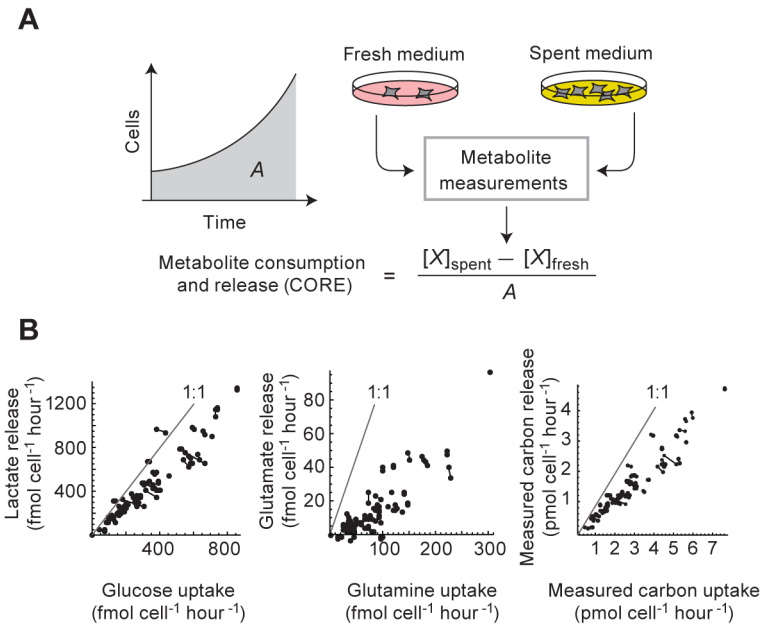

Figure 1. Metabolite consumption and release (CORE) profiling

A: For determining metabolite CORE (consumption and release rate) profiles, medium samples taken before (fresh) and after (spent) 4–5 days of cell culture are subjected to metabolite profiling using LC-MS/MS. For each metabolite *X*, the CORE value is calculated as the difference in molar abundance normalized to the area *A* under the growth curve. B: Glucose consumption vs. lactate release; glutamine consumption vs. glutamate release; and total measured carbon consumption vs. total measured carbon release, across the 60 cell lines. Gray lines indicate the 1:1 molar ratio of carbon consumed: carbon released for each metabolite pair; joined data points represent biological replicates.

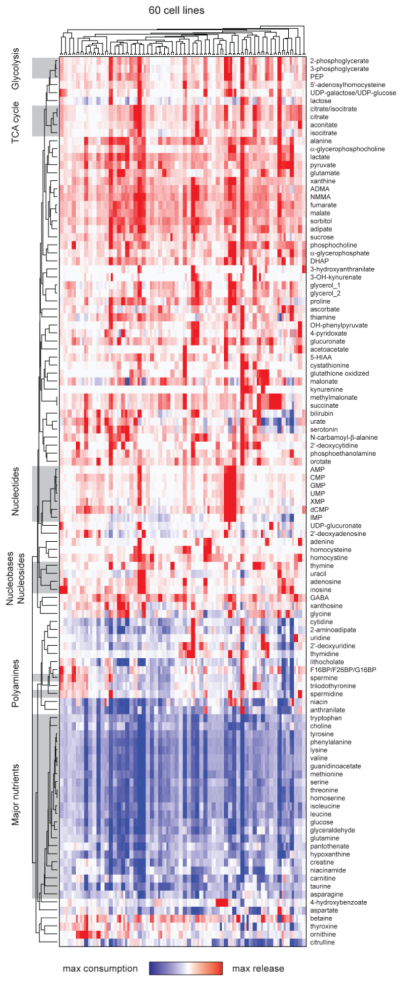

Figure 2. CORE profiling across the NCI60 cell lines

Hierarchical clustering of CORE profiles for 111 metabolites across 60 cancer cell lines, in duplicate cultures. Blue color indicates consumption, white indicates no change, and red color indicates release. Gray highlights indicate functionally related metabolites. Metabolites that cannot be distinguished are denoted as x/y. Glycerol_1 and glycerol_2 represent independent LC-MS/MS measures.

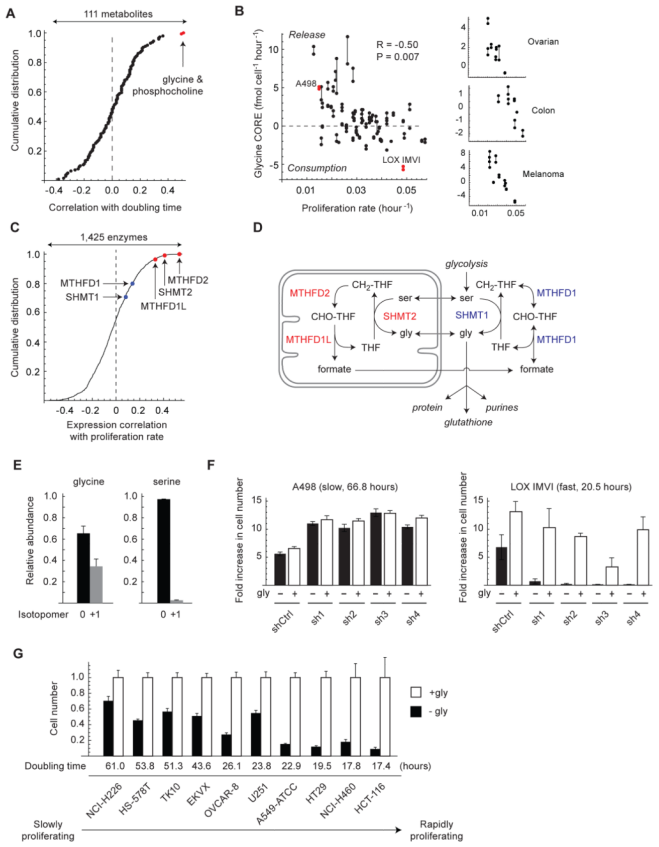

Figure 3. Glycine consumption and synthesis are correlated with rapid cancer cell proliferation

A: Distribution of Spearman correlations between 111 metabolite CORE profiles and proliferation rate across 60 cancer cell lines. Metabolites highlighted in red are significant at $P < 0.05$, Bonferroni-corrected. B: Glycine CORE versus proliferation rate across 60 cancer cell lines (left) and selected solid tumor types (right). Cell lines selected for follow-up experiments are highlighted in red. Joined data points represent replicate cultures. P-value is Bonferroni-corrected for 111 tested metabolites. C: Distribution of Spearman correlations between gene expression of 1,425 metabolic enzymes and proliferation rates across 60 cancer cell lines. Highlighted are mitochondrial (red) and cytosolic (blue) glycine metabolism enzymes. D: Schematic of cytosolic and mitochondrial glycine metabolism. E: Abundance of unlabeled (0) and labeled (+1) intracellular glycine and serine in LOX IMVI cells grown on 100% extracellular ^{13}C-glycine. F. Growth of LOX IMVI and A498 cells expressing shRNAs targeting SHMT2 (sh1-4) or control shRNA (shCtrl), normalized to shCtrl cells; gly, glycine. G. Growth of 10 cancer cell lines expressing shRNA targeting SHMT2 (sh4) after 3 days cultured the absence (−gly, filled bars) or presence (+gly, open bars) of glycine. Cell number is presented as a ratio relative to +gly cells. Error bars in E,F,G denote standard deviation.

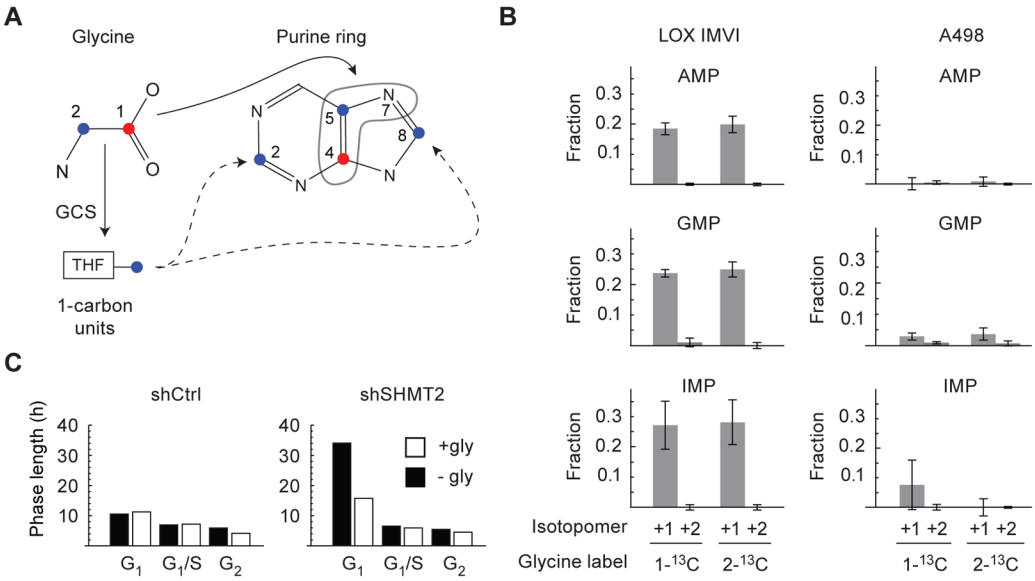

Figure 4. Glycine metabolism supports *de novo* purine nucleotide biosynthesis

A: Schematic of carbon incorporation into the purine ring from 1-^{13}C-glycine or 2-^{13}C-glycine; THF, tetrahydrofolate; GCS, glycine cleavage system. B: Purine nucleotide +1 and +2 isotopomers in LOX IMVI or A498 cells grown on 100% 1-^{13}C-glycine or 2-^{13}C-glycine, as a fraction of the total intracellular metabolite pool. C. Cell cycle analysis in HeLa cells expressing shRNA targeting SHMT2 (shSHMT2) or control shRNA (shCtrl), grown in the absence (−gly, filled bars) or presence (+gly, open bars) of glycine. Cell cycle phase length was calculated from the percentage of cells present in each cell cycle phase by geminin expression and DAPI staining (Fig. S11C).

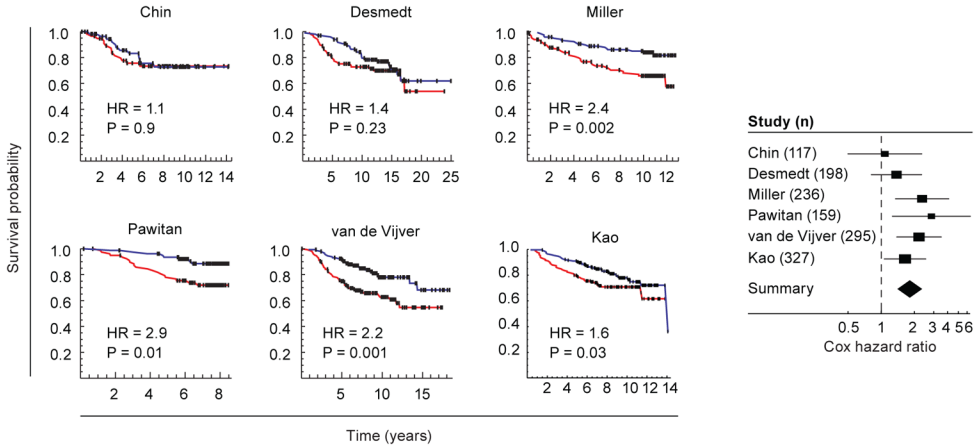

Figure 5. Expression of the mitochondrial glycine biosynthesis pathway is associated with mortality in breast cancer patients

Left, Kaplan-Meier survival analysis of six independent breast cancer patient cohorts (22–27). Patients were separated into above (red line) and below (blue line) median expression of mitochondrial glycine metabolism enzymes (*SHMT2*, *MTHFD2*, and *MTHFD1L*, Fig. 3D). Dashes, censored events. Right, meta-analysis of Cox hazard ratios for the six studies. Solid lines denote 95% confidence intervals; boxes denote the relative influence of each study over the results (inverse squared standard error). Diamond marks the overall 95% confidence interval.